The 9th International Symposium on Virtual Reality, Archaeology and Cultural Heritage VAST (2008)
M. Ashley, S. Hermon, A. Proenca, and K. Rodriguez-Echavarria (Editors)

A Comparison on Features Efficiency in Automatic Reconstruction of Archeological Fragmented Objects

D. F. Soldea, O. Soldea, G. Unal, and A. Ercil

Sabancy University, Orhanli, Tuzla, Istanbul, Turkey

Abstract

Automatic reconstruction of archeological fragmented objects is an invaluable tool for restoration purposes and personnel. In this paper, we assume that broken pieces resemble similar characteristics on their common boundaries, when they are correctly combined, of course. Bearing in mind that common boundaries preserve texture and geometry, we analyze features that allow the transport of characteristics over the common boundaries. We present a quantitative and qualitative comparison over a large set of features and over a large set of synthetic and real archeological fragmented objects. To the best of our knowledge, this is the first work that provides evidences for the most utile features.

Categories and Subject Descriptors (according to ACM CCS): I.4.3 [Image Processing]: Registration I.4.5 [Image Processing]: Reconstruction I.4.7 [Image Processing]: Feature measurement,Feature representation, Moments, Texture I.4.9 Archeologic reconstructionApplications

1. Introduction

Reconstruction of archeological pieces from fragments of parts found in archeological sites is a long time task if it is manually performed. In order to help the archeologists and reconstruction personnel, several automatic tools for the reconstruction of fragmented archeological pieces were developed until now.

The reconstruction algorithms, usually, read from the input images of fragmented pieces and provide to the output positions for the fragmented pieces. For example, Fig. 1 shows a typical input fragmented image. Figure 1 (c) shows a possible reconstruction outcome, that was obtained employing [SE] and [SE05].

The idea of matching two or more pieces in automatic reconstruction of archeological fragmented objects is that common features of neighbors are more strongly related than the others. For example, in [SE], [SE05], the authors propose a method that begins with expanding each input piece outwards, by predicting the pictorial information of the outer space, a process which is also known as inpainting [BBS01], [Wei99], [Tsc06], [Tel04]. In addition, features values are derived from the input pieces as well as from the inpainted regions. An affinity measure of corresponding pieces is defined and alignment of the puzzles pieces is carried out using an FFT based image registration technique. The optimization of total affinity gives the best assembly of the fragmented pieces. We will refer to the assembly of fragmented pieces by the term puzzle.

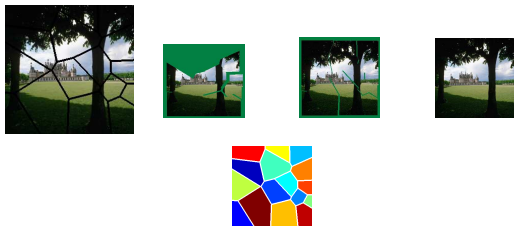

Figure 1: *Example of reconstruction of fragments using different features (a) a fragmented image, (b) the reconstructed image using the mean of the gray scale component, (c) The reconstructed image using the mean of the Y, Cb, Cr channels, (d) a synthetic image, and (e) a mask for fragmenting simulation.*

The selection of a feature extraction method from texture exactly depends on the samples of the pieces. For example, the statistical method (histogram statistics) is better in a jigsaw puzzle. On the other hand, the structural methods (laplacian in a window) are more reasonable in a painting including directional lines on an archaeological fragment. Furthermore, we experimentally verified that the features involved in several automatic reconstruction schemes influence the accuracy of results. A natural question that arose in these experiments is what are the best features to be used in the context of automatic reconstruction of archeological fragmented objects? In this context, Fig. 1 (b) and (c) show different possible outcomes for reconstruction, that were obtained using the mean of grayscale and the mean of the luminance and chrominance channels (YCbCr) of the fragments in Fig. 1 (a).

In order to answer this challenging problem, we present a quantitative and qualitative comparison over a large set of features and over a large set of synthetic and real archeological fragmented objects. To the best of our knowledge, this is the first work that provides evidences for the most utile features. Most of the features used are local ones and can be computed from small neighbors bands. In addition, we also propose a set of curvature field based features. A curvature field is evaluated by sampling a continuous B-spline [IRI] field. The curvature field serves as an input image, on top of which other features are evaluated.

2. Features

In this section, we describe the features that we analyze. We compute the mean, the median, the variance, and the canonical moments (up to order six). Each of these features is computed over a mask of n x n neighbor pixels. We also compute the normal curvature of the iso-lines field. The computation of the curvature based feature is conducted via B-spline functions evaluation and its proposed use towards automatic reconstruction is explained separately.

Consider a region of n x n pixels indexed by $I_{x,y}$, where $x,y \in \{-1,0,1\}$. $I_{x,y}$ is a neighborhood of pixels that enables the computation of features for $I_{0,0}$.

2.1. Mean, Median, and Variance

Define the mean as $\mu_I = \frac{1}{9}\sum_{i=-1}^{1}\sum_{j=-1}^{1} I_{i,j}$. The variance is $\sigma_I^2 = \frac{1}{8}\sum_{i=-1}^{1}\sum_{i=-1}^{1}(I_{i,j}-\mu_I)^2$. The median is defined as the value with same number of observations preceding it, and following it, in the 3x3 neighborhood.

2.2. Moments

Assume $f(x,y)$ is a distribution function, i.e. $f(x,y)$ is the value of the continuous image at (x,y). For the discrete case, $f(x,y)$ represents the value of the pixel (x,y). Following [PR92], we define the continuous standard moments as $m_{pq} = \int\int_{\Omega} x^p y^q f(x,y)dxdy$, where Ω is the domain of definition of an analyzed object. The discrete moments of the 3x3 neighborhood $I_{x,y}$, (where $x,y \in \{-1,0,1\}$), are $m_{pq} = \sum_{y=-1}^{1}\sum_{x=-1}^{1} x^p y^q I_{x,y}$, for $p,q = 0,1,2,....$ In the discrete case we consider $\Omega = I_{x,y}$, which is the 3x3 neighborhood, and regard it as an analyzed object. Using the moments of order one, we can find the center of the mass of the analyzed objects. Using moments of order up to two one can find the canonic orientation of the analyzed object. Consider an analyzed object that its center of mass is located in the origin of the coordinate axes and its orientation is canonical. We call the moments that are computed for such an object the canonic moments of the analyzed object. They are intrinsic to the shape. For clarity, when computing canonic moments we obtain $m_{10} = m_{01} = m_{11} = 0$.

2.3. Curvature Field

In this section we define and describe the computation of the curvature field of an image that we implemented. Let $I_{x,y}$ be the values of the pixels of the input image, where $x \in \{0..m\}$ and $y \in \{0..n\}$. Following [SER06], we model the image $I_{x,y}$ as a continuous field represented by an uniform open-end cubic B-spline surface $f(x,y) = \sum_{i=0}^{n}\sum_{j=0}^{m} I_{x,y} B_{i,3,\tau_x}(x) B_{j,3,\tau_y}(x)$, where τ_x and τ_y are (uniform) knots. The knots are defined such that the domain of definition of the B-spline surface fits exactly the domain of the input image. We symbolically compute B-spline surfaces of the first and second derivatives of $f(x,y)$. For each pixel (x,y), we evaluate the derivatives $f_x, f_y, f_{x,x}, f_{x,y}$, and $f_{y,y}$, and assign $Kn_{x,y} = -sign(f_y)\frac{f_{x,x}f_y^2 - 2f_{x,y}f_xf_y + f_{y,y}f_x^2}{\sqrt{(f_x^2+f_y^2)^3}}$, where the derivatives are evaluated at the (x,y) parametric location and $sign(z)$ means the sign of the z value.

The resulting Kn has the same dimension as I and represent the values of the normal curvatures of iso-lines of I. Mainly, we followed the line of symbolic computations of the Gaussian and mean curvature in [SER06], however, we decided to move part of the computations into the discrete domain due to computation time reasons. Figures 2 (a) and (b) represent an input image and its curvature field respectively.

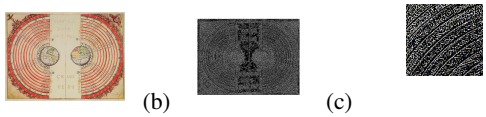

Figure 2: *(a) An archeological image, (b) the curvature field of the image in (a), and (c) a cropped region from the curvature field.*

3. Matching Two Fragments for Grading

In this section, we describe the grading procedure of the features when matching fragments that are automatically generated or are achieved from real fragmented objects. The automatic fragmentation procedure is conducted via masks (to be illustrated and defined next), it is described in Section , and we assume that we have a large set of such masks here. Fig. 1 (e) shows a segmentation mask. This mask, when applied on Fig. 1 (d) produces the fragments shown in Fig. 1 (a).

Consider the archeological basrelief image in Fig. 3 (a). We automatically generate masks for fragmentation such as the one shown in Fig. 3 (b). In Fig. 3 (b), the red region defines the fragment shown in Fig. 3 (c) (including the L_1 region, to be explained in the following). Fig. 3 (d) (without the L_2 region) represents the fragment as defined by the blue region in Fig. 3 (b). The L_2 region is an inpainted region, which for simulation purposes is taken from the original image Fig. 3 (a) as is. In the context of our measurements, L_2 is a simulation of the inpainting results when working on automatically generated masks. When working on physically fragmented archeological objects, L_2 results from inpainting, of course. We employ Crisini for inpainting purposes. The inpainting procedure naturally produces confidence maps, the largest the inpating is the lower the confidence of reproduction is. Confidence maps are used towards weights evaluation in grading. We simulate confidence maps in terms of distance maps. Figures 3 (e) and 3 (f) show the confidence maps for the fragments in Fig. 3 (b) and (c) respectively.

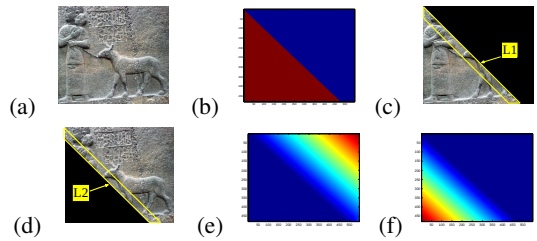

Figure 3: *(a) An archeological image, (b) a mask for fragmenting (c) and (d) two fragments of an image, (e) and (f) two distance map example.*

For each one of the fragments, the following procedure can be repeated. Consider the fragment in Figure 3 (d) fixed and inpainted with the L_2 region. For every pixel in L_2 we compute each one of features described in Section 2. Denote a pixel in L_2 by x,y. Moreover, the other fragment, which is depicted in Figure 3 (c) is translated with at most one pixel in each possible direction. For each such translation, the pixel x,y is compared versus an eventual neighbor from Figure 3 (c). Therefore, the features of the pixel x,y have up to nine counterparts from the floating fragment Figure 3 (c). Denote the a feature of x,y by f and its counterparts with $f_{i,j}, i,j \in \{-1,0,1\}$.

The affinity between the pixel x,y with its translated counterpats is calculated with the following formula:

$$error = \frac{1}{25} \sum_{j=-2}^{2} \sum_{i=-2}^{2} \frac{|f_{i,j} - f_0|}{|f_{i,j}| + |f_0|} \quad (1)$$

In function of the error value, we can give a score for every pixel (see Table (1)).

Table 1: *Measure of the affinity between two pixels*

error	score
$10^{-5} < error < 10^{-4}$	10
$10^{-4} < error < 10^{-3}$	9
$10^{-3} < error < 10^{-2}$	8
$10^{-2} < error < 10^{-1}$	7
$10^{-1} < error < 1$	6
$1 < error < 10$	5

We compute a global score for every fragment from image, by averaging all the scores of the pixels in the corresponding inpainting region. This average is weighted using a distance map, pixels closer to the original image receiving higher weights. The corresponding weight is choose by $weight_k = exp(-distmap(k)/\sigma)$, where σ is a constant. Experimentally, we choose $\sigma = 1000$. The global score per fragment of image is computed by $score_{global} = \sum_k score_k * weight_k$. We compute the average of all the global score corresponding to the fragments from every image. Finally, a average of global scores on all the images is performed. In the next section are presented the experiments performed and the results obtained.

4. Experiments

A number of 25 images, synthetic and real (archeological) images are used in the simulations (see Fig. 4). On every image are applied, consecutively, masks of 4, 8, and 16 fragments. The features are computed over grayscale, RGB, and YCbCr representations of images. A average of every feature for all the fragments from a image and a average of every feature over all the images is performed.

In Table 2, are indicated a number of features and the global grades obtained for them.

In Table 3, are indicated the best features obtained for a set 6 images from all the 25 images used in experiments and the best feature resulted for the entire set of image.

In Fig. (5) the graphics represents the score obtained for every feature used in computation. The features are sorted in a decreasing order, from the best feature the the worst feature.

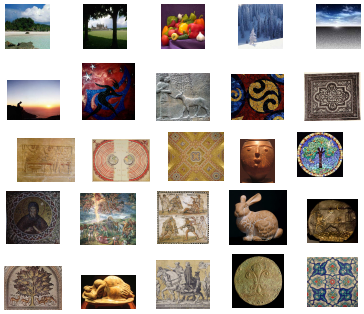

Figure 4: *Examples of synthetic and real images*

Table 2: *Global grades for a number of features*

-	Gray	R	G	B	Y	Cb	Cr
Mean	0.09	0.09	0.09	0.09	0.09	0.1	0.1
Median	0.08	0.07	0.07	0.07	0.08	0.07	0.07
Variance	0.08	0.08	0.08	0.08	0.08	0.08	0.08
m_{00}	0.09	0.09	0.09	0.09	0.09	0.1	0.1
m_{02}	0.08	0.08	0.08	0.08	0.08	0.1	0.1
m_{20}	0.09	0.09	0.09	0.09	0.09	0.1	0.1
m_{03}	0.08	0.08	0.08	0.08	0.08	0.08	0.08
m_{12}	0.08	0.08	0.08	0.08	0.08	0.08	0.08
m_{21}	0.08	0.08	0.08	0.08	0.08	0.08	0.08
m_{30}	0.08	0.08	0.08	0.08	0.08	0.08	0.08

The first best twenty features are: mean of component Cr, m_{00} of component Cr, mean of component Cb, m_{00} of component Cb, m_{02} of component Cr, m_{20} of component Cr, m_{02} of component Cb, m_{20} of component Cb, m_{04} of component Cr, m_{40} of component Cr, m_{04} of component Cb, mean of component Y, m_{00} of component Y, m_{40} of component Cb, m_{20} of component Y, mean of gray scale component, m_{00} of gray scale component, mean of G component, m_{00} of component G, and m_{20} of gray scale component.

Finally, we use two different features in the process of reconstruction of two images archeological images. From Fig. 6, we can see that, the best results of reconstruction are obtained when are used features with the high scores, i.e., mean Cr, mean Cb, and mean Y.

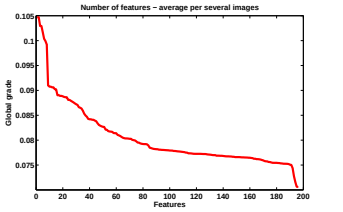

Figure 5: *Graph with global grades per feature*

Table 3: *Best features, for 25 images and fragments of 4, 8, 16 in the every image*

-	4 pieces per mask	8 pieces per mask	16 pieces per mask
Im_1	mean Cr 0.15	mean Cr 0.11	mean Cr 0.07
Im_2	mean Cr 0.15	mean Cr 0.11	mean Cr 0.07
Im_3	mean Cr 0.13	mean Cr 0.1	mean Cr 0.06
Im_4	mean Cr 0.14	mean Cr 0.1	mean Cr 0.07
Im_5	mean Cb 0.15	mean Cb 0.11	mean Cb 0.07
.....	.....	.....	.....
Im_{25}	mean Cb 0.15	mean Cb 0.11	mean Cb 0.07
Total	mean Cr 0.14	mean Cr 0.11	mean Cr 0.07

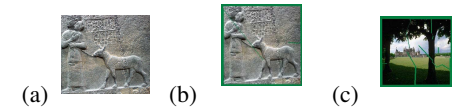

Figure 6: *Example of reconstruction of fragments using different features (a) A synthetic image, (b) a mask for fragmenting, (c) a fragmented image (d) The reconstructed image using as feature the mean of components, R,G,B, and (e) The reconstructed image using as feature the mean of components, Y, Cb, Cr.*

4.1. 2D Breaker Simulator

In the experiments it is used a 2D breaker. The algorithm for 2D breaker simulator is based on radial functions. This algorithm has as input, the following parameters: the dimensions of the mask, and N, the number of broken pieces. The output parameter is a mask with N different labeled regions. The steps of the algorithm are described in the following:

1. Choose randomly N number of points on the image
2. Apply a random distribution around each of the points previously chosen
3. Label the N regions using maximum values criterion
4. Create continue labeled regions
5. Apply erosion on the margins of the regions
6. Verify the continuity of the labels and re-label the regions if it is necessary

In Fig 7 are shown several examples of mask with fragments of 4, 8, 16, and 32.

5. Conclusions

In this article was simulated a system that provide a score for number of features. Several formats of images were used:

Figure 7: *Example of mask with 4,8,16 and 32 pieces*

gray scale, RGB, and YCbCr. The best features obtained are related to the YCbCr's format.

References

[BBS01] BERTALMIO M., BERTOZZI A. L., SAPIRO G.: Navier stokes fluid dynamics and image and video inpainting. *"Proc.of Conf. Computer Vision Pattern Recognition" 12*, 3 (2001), I:355–365.

[IRI] http://www.cs.technion.ac.il/∼irit/.

[PR92] PROKOP R. J., REEVES A. P.: A survey of moment-based techniques for unoccluded object representation and recognition. *"CVGIP" 12*, 3 (1992), I:355–365.

[SE] SAGIROGLU M. S., ERCIL A.: A texture based matching approach for automated assembly of puzzles. *"ICPR2006"*.

[SE05] SAGIROGLU M. S., ERCIL A.: A texture based approach to puzzle assembly. *"VAST 2005" 12*, 3 (July 2005), 251–276.

[SER06] SOLDEA O., ELBER G., RIVLIN E.: Global segmentation and curvature analysis of volumetric data sets using trivariate b-spline functions. *"TPAMI" 28*, 2 (2006), 265–278.

[Tel04] TELEA A.: An image inpainting technique based on the fast marching method. *"Journal of Graphics Tools" 9*, 1 (2004), 23–34.

[Tsc06] TSCHUMPERLE D.: Fast anisotropic smoothing of multi-valued images using curvature-preserving pde's. *"International Journal of Computer Vision" 68*, 1 (2006), 65–82.

[Wei99] WEICKERT J.: Coherence-enhancing diffusion of color images. *"Image Vis. Comput." 17*, 3-4 (1999), 201–212.